INTERNATIONAL JOURNAL FOR NUMERICAL AND ANALYTICAL METHODS IN GEOMECHANICS, VOL. 13, 531–550 (1989)

A SEMI-ANALYTIC MODEL FOR CONTAMINANT MIGRATION IN A REGULAR TWO- OR THREE-DIMENSIONAL FRACTURED NETWORK: CONSERVATIVE CONTAMINANTS

R. K. ROWE

Geotechnical Research Centre, Faculty of Engineering Science, The University of Western Ontario, London, Canada N6A 5B9

AND

J. R. BOOKER

School of Civil and Mining Engineering, The University of Sydney, Sydney, Australia

SUMMARY

A new semi-analytical solution for the transport of a conservative contaminant species in a fractured medium having a regular two- or three-dimensional fracture network is presented. The application of the technique and some of the practical implications arising from an examination of contaminant migration in fractured systems is discussed. Particular consideration is given to the effects of Darcy velocity, fracture spacing, matrix porosity, dispersivity and the mass of contaminant available for transport. The implications of uncertainty with respect to fracture opening size and ground-water velocity is also discussed and it is shown that provided one can obtain a reasonable estimate of the hydraulic gradient and hydraulic conductivity for the rock mass, uncertainty regarding the magnitude of the opening size and the groundwater velocity does not have a significant effect on predicted contaminant migration for the class of problems being considered.

INTRODUCTION

Fractured porous media are frequently encountered adjacent to present or proposed waste disposal facilities. These fractured media may, for example, take the form of fractured till with predominantly vertical fractures or of a fractured rock (e.g. mudstone, siltstone, sandstone) which has significant horizontal and vertical fracturing. Since the fracture opening size is generally quite small, so too is the effective fracture porosity, n_b, with a typical range of between 10^{-2} and 10^{-5}.[1] As a consequence, the groundwater velocity, v_f, may be quite high and the potential for rapid contaminant migration along these fractures is a source of concern in the evaluation of the potential impact of these facilities upon ground-water quality.

Over the past 30–40 years numerous landfills have been constructed in fractured soil or rock, and in many cases contaminant transport has been quite limited even though ground-water velocities may be of the order of tens to hundreds of metres per year. This implies that the velocity of contaminant transport is substantially less than the groundwater velocity. Several investigators have attributed this phenomenon to the attenuation of contaminants which can result from diffusion of contaminants from the fractures into the porous matrix adjacent to the fractures.[1–5]

Finite-element techniques provide one means of modelling contaminant migration in fractured systems.[2,6] These approaches potentially make it possible to analyse quite complicated two- (and

0363–9061/89/050531–20$10.00

Received 15 March 1988
Revised 23 December 1988

possibly three-) dimensional fracture networks. However, these approaches are most useful when there is detailed data available concerning the distribution and characteristics of the fracture system. Frequently, these data are not available and it is necessary to assess potential impact based on a knowledge of typical fracture spacings and orientations together with some knowledge of the hydraulic characteristics of the system (i.e. hydraulic gradient and hydraulic conductivity). Under these circumstances, analytic or semi-analytic solutions for contaminant transport in a fractured medium may be particularly useful for quickly assessing the potential effects of uncertainty regarding key parameters (e.g. fracture spacing, fracture opening size, etc.). These techniques may also be useful for bench-marking more complex numerical procedures (e.g. finite-element codes).

Various investigators have developed analytical or semi-analytical solutions for contaminant transport in idealized fracture media. For example, Neretnicks[7] and Tang *et al.*[8] developed a solution for one-dimensional (1D) contaminant transport along a single fracture together with 1D diffusion of contaminant into the matrix of the rock adjacent to the fracture. Sudicky and Frind[9] and Barker[10] extended this approach to consider the case of multiple parallel fractures. The aforementioned researchers all considered constant concentration at the inlet of the fractures. Moreno and Rasmuson[11] developed an analytical equation for a constant flux boundary condition at the inlet of a single fracture.

Rowe and Booker[12] considered the situation that is encountered with landfills wherein there is a finite mass of contaminant available for transport into the ground-water systems. In these situations, it may be expected that the concentration of contaminant in the source (landfill) will decrease with time as mass is transported into the fracture network. Thus the authors' previous solution considers a variable inlet concentration for a series of parallel fractures. In this model, the concentration at the source (inlet) was obtained from consideration of conservation of mass and the finite initial mass of contaminant available for transport.

The analytic and semi-analytic solutions noted above all considered a single plane of fracturing. This then leaves open the question as to what effect a second or third direction of fracturing may have on contaminant transport?

The objective of this present paper is to present a semi-analytical solution for contaminant migration in a fractured medium having a regular two- or three-dimensional fracture network. This solution will consider the effect of a finite mass of contaminant. The implications of considering a two- or three-dimensional, as opposed to one-dimensional, system will be discussed, and the influence of a number of key parameters (such as diffusion coefficient, matrix porosity, fracture porosity, dispersivity, groundwater velocity and Darcy velocity) will be examined for conservative contaminant species. (The migration of reactive species will be discussed in a subsequent paper.)

DEVELOPMENT OF THEORY

Consider an extensive landfill which is adjacent to fractured ground. It will be assumed that there are three possible sets of planar fissures. Referring to Figure 1, suppose that Ox, Oy, Oz is a set of Cartesian reference axes; it will be assumed that the first set of fissures are a distance $2H_1$ apart, of width $2h_1$, and parallel to the xy plane; the second set of fissures is assumed to be spaced at an interval of $2H_2$, of width $2h_2$ and parallel to the xz plane; the third set of fissures is assumed to be spaced at an interval $2H_3$, of width $2h_3$ and parallel to the zy plane. The ground adjacent to the landfill is thus assumed to consist of a series of rectangular blocks made up of a homogeneous matrix material separated by fissures having a width far smaller than the smallest dimension of the box.

It will be assumed that the interface of the landfill and the adjacent ground is the yz plane ($x=0$)

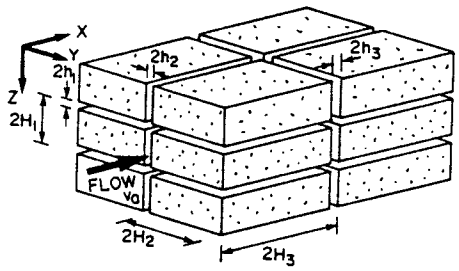

Figure 1. Definition of fracture geometry

and that the landfill is quite extensive so that the predominant mechanism for transport of the leachate will be one-dimensional advective–dispersive transport along fissure sets 1 and 2 accompanied by some diffusion of leachate into the intact blocks.

It now follows from a consideration of conservation of mass and assuming that the initial concentration of leachate in the fissures is zero, that

$$\int_0^t \left(\frac{h_1}{H_1} \frac{\partial F_1}{\partial x} + \frac{h_2}{H_2} \frac{\partial F_2}{\partial x} \right) dt + q + \left(\frac{h_1}{H_1} + \frac{h_2}{H_2} + \frac{h_3}{H_3} \right) c_f = 0 \tag{1}$$

where F_1 is the flux in fissure set 1, F_2 is the flux in fissure set 2, q is the mass of leachate/unit volume entering the intact matrix and c_f is the concentration of leachate in the fissures.

The transport of leachate along the fissure sets 1 and 2 is governed by

$$F_1 = v_1 c_f - D_1 \frac{\partial c_f}{\partial x}$$

$$F_2 = v_2 c_f - D_2 \frac{\partial c_f}{\partial x} \tag{2}$$

where v_1, v_2 denote the velocities of the ground water in the x direction in fissure sets 1 and 2, respectively, and D_1, D_2 denote the coefficients of hydrodynamic dispersion (incorporating the effects of molecular diffusion and mechanical dispersion) in fissure sets 1 and 2, respectively.

If equations (1) and (2) are combined it is found that

$$\int_0^t \left(D_a \frac{\partial^2 c_f}{\partial x^2} - v_a \frac{\partial c_f}{\partial x} \right) dt = n_f c_f + q \tag{3}$$

where it has been convenient to introduce the Darcy velocity

$$v_a = \frac{h_1}{H_1} v_1 + \frac{h_2}{H_2} v_2 \tag{4a}$$

and the apparent coefficient of hydrodynamic dispersion

$$D_a = \frac{h_1 D_1}{H_1} + \frac{h_2 D_2}{H_2} \tag{4b}$$

and the total fissure porosity

$$n_f = \frac{h_1}{H_1} + \frac{h_2}{H_2} + \frac{h_3}{H_3} \tag{4c}$$

For the special case where the groundwater velocity is the same in both fracture sets (i.e. $v_f = v_1 = v_2$), equations (4a) and (4b) reduce to

$$v_a = n_b v_f \tag{5a}$$

$$D_a = n_b D \tag{5b}$$

where

$$n_b = \frac{h_1}{H_1} + \frac{h_2}{H_2} \tag{5c}$$

It is also noted that the coefficient of hydrodynamic dispersion along the fractures may often be related to the groundwater velocity v_f and the dispersivity α. Thus, for example,

$$D = \alpha v_f \tag{6a}$$

and hence (5b) would reduce to

$$D_a = n_b \alpha v_f \tag{6b}$$

The dispersivity α, is often taken to be a function of the travel distance, at least until the travel distance is large compared with the non-homogeneities which give rise to the dispersion process.[13]

A Laplace transform, namely

$$\bar{c}_f = \int_0^\infty e^{-st} c_f \, dt \tag{7}$$

can be used to eliminate time from equation (3), and it is found that

$$\frac{1}{s}\left(D_a \frac{\partial^2 \bar{c}_f}{\partial x^2} - v_a \frac{\partial \bar{c}_f}{\partial x}\right) = n_f \bar{c}_f + \bar{q} \tag{8}$$

The form of q is examined in the Appendix and it is shown that $\bar{q}$ can always be expressed in the form

$$\bar{q} = s\bar{\eta}\bar{c}_f \tag{9}$$

where $\bar{\eta}$ is a known function of the Laplace transform variable and is given in the Appendix. It thus follows that

$$D_a \frac{\partial^2 \bar{c}_f}{\partial x^2} - v_a \frac{\partial \bar{c}_f}{\partial x} = s(n_f + \bar{\eta})\bar{c}_f \tag{10}$$

It is now assumed that the length of each of the fissures constituting sets 1 and 2 is far greater than the minimum spacing between adjacent fissure planes, and thus that the solution of equation (10) must vanish as $x \to \infty$. It therefore follows that

$$\bar{c}_f = \bar{c}_{LF} e^{-\omega x} \tag{11}$$

where c_{LF} is the concentration in the landfill and

$$\omega = \frac{-v_a + [v_a^2 + 4D_a s(n_f + \bar{\eta})]^{1/2}}{2D_a}$$

Now suppose that initially the concentration of leachate in the landfill is $c_{LF}(0) = c_0$, and that the area of contact between the landfill and the adjacent ground is A, then assuming that the volume V of leachate in the landfill remains constant but that its concentration diminishes, it follows from

conservation of mass that

$$V c_{LF}(0) - V c_{LF}(t) + A \int_0^t F \, dt = 0$$

where $F = F_1 + F_2$ (where F_1, F_2 are defined by equation (2)) denotes the flux entering the fissured ground from the landfill.

It now follows upon application of a Laplace transform and introducing the equivalent height of leachate $H_f = V/A$ that

$$\frac{c_{LF}(0)}{s} = \bar{c}_{LF} + \frac{1}{sH_f}(v_a + \omega D_a)\bar{c}_{LF} \tag{12}$$

and thus

$$\bar{c}_{LF} = \frac{c_{LF}(0)}{\left[s + \left(\frac{v_a + \omega D_a}{H_f}\right)\right]} = \frac{c_0}{\left[s + \frac{v_a + \omega D_a}{H_f}\right]} \tag{13}$$

The solution is now complete in Laplace transform space; the solution in the time domain can be found by numerical inversion using the efficient algorithm developed by Talbot.[14]

For convenience of presentation, the initial concentration in the landfill will be denoted by c_0 in the following section.

RESULTS

To illustrate the application of the theory described in the previous section, consideration will be given to the migration of a conservative contaminant in a fractured rock for the range of parameters given in Table I. Conservative contaminants are contaminants which remain in solution and are not attenuated by processes such as sorption (e.g. due to cation exchange or partitioning with organic matter in the rock matrix), radioactive decay, biological action or chemical precipitation. A common example is chloride.

Table I. Parameters considered in this study (the italicized value indicates the value used unless otherwise noted)

Parameter	Symbol	Value(s)
Darcy velocity (m/a)*	v_a	0·04, *0·08*
Fracture spacing (m)	$2H_1$	*0·05*, 0·5
	$2H_2$	*0·05*, ∞
	$2H_3$	*0·05*, ∞
Fracture opening size (μm)	$2h_1$	*10*, 20, 40
	$2h_2$	*10*, 20, 40
	$2h_3$	*10*, 20, 40
Fracture porosity of the plane perpendicular to flow	$n_b = [(h_1/H_1 + h_2/H_2)]$	*0·004*, *0·0008*
Groundwater velocity (m/a)*	v_f	50, *100*, 200
Diffusion coefficient in rock matrix (m^2/a)*	D_m	0·0018, 0·0036
Porosity of rock matrix	n_m	0·05, 0·1
Dispersivity (m)	α	*0·03*, 0·3, 1·5, 3·0, 6
Height of leachate (m)	H_f	0·1, *1*, 10, ∞

* Note: 'a' denotes "annum", i.e. year

Finite mass of contaminant

The importance of considering the finite mass of contaminant available for transport into the hydrogeological system has been discussed by Rowe[5] for a number of contaminant migration problems. The effect is equally important when considering migration through a three-dimensional fractured system. For example, Figure 2 shows the calculated concentration plume downgradient of a hypothetical landfill after 30 years migration for heights of leachate, H_f, of 0·1 m, 1 m, 10 m and ∞. An infinite height of leachate ($H_f = \infty$) corresponds to the case where the source concentration remains constant for all time. When a finite mass of contaminant is considered, the concentration in the source decreases with time and the peak concentration moves along the fracture system being attenuated by the process of matrix diffusion with increasing distance from the source.

The smaller the initial mass of contaminant available for transport, the greater the potential attenuation due to diffusion of contaminant into the rock matrix. After 30 years migration for the conditions shown in Figure 2, the peak concentration for $H_f = 10$ m is about 96 per cent of the original source concentration and occurs at a point about 41 m from the source, whereas the source concentration has decreased to about 79 per cent of its original value. In contrast, for $H_f = 0{\cdot}1$ m, the peak concentration has reduced to about 25 per cent of the original source value and occurs at a point about 46 m from the source. For this latter case, the plume is largely restricted to a zone between 35 and 55 m from the source. The intermediate case of $H_f = 1$ m has a peak of about 76 per cent of the initial source value at a point 43 m from the source, whereas the source value itself has reduced to about 9 per cent of its original value. A value of $H_f = 1$ m will be adopted for the remainder of this paper.

In evaluating the rate of advance of a contaminant plume, care is needed in interpreting the meaning of the time at which the contaminant front or peak impact arrives at a given point. For example, in examining Figure 2 it is evident that after 30 years migration the peak of the contaminant front is most advanced for $H_f = 0{\cdot}1$ m (i.e. the distance to the peak is 46 m from the source for $H_f = 0{\cdot}1$ m compared to 43 m for $H_f = 1$ m and only 41 m for $H_f = 10$ m). Thus, the

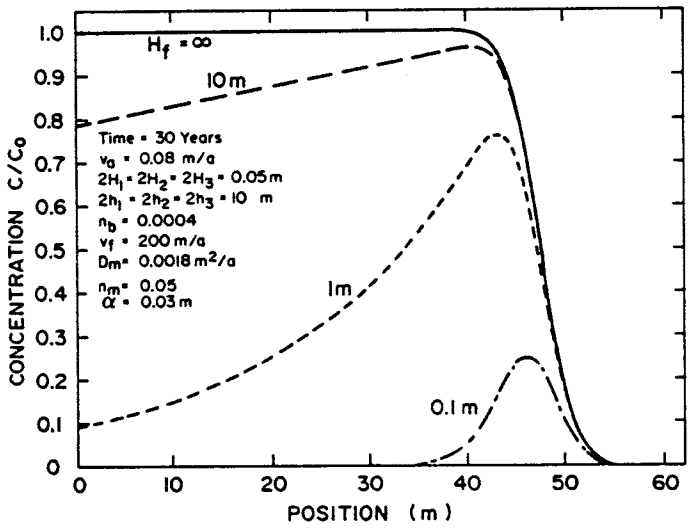

Figure 2. Effect of the equivalent height of leachate H_f on the contaminant plume: 3D analysis

peak concentration appears to be moving faster for the lower mass of contaminant, however inspection of Figure 2 also clearly shows that the impact at any location is greater the greater the masses of contaminant. Thus, although the peak of the contaminant plume is at 46 m after 30 years for $H_f = 0{\cdot}1$, the impact at this location and time is even greater for $H_f = 1$ m or 10 m even though the maximum impact for the higher masses of contaminant has not yet occurred at the 46 m point after 30 years. Furthermore, Figure 2 also shows that the front of the contaminant plume (defined here as the most distant point at which the increase in concentration $c = 0{\cdot}1\ c_0$) does move fastest for a high mass of contaminant. The primary point to be emphasized being that *both* the impact and the velocity of the contaminant plume are related to the available mass of contaminant and one must be careful not to extrapolate the results for a given mass of contaminant to infer what might be the results for a different mass of contaminant.

It is noted in passing that the results presented in Figure 2 are for a groundwater velocity of 200 m/a (metres/annum; metres/year), however the velocity of the contaminant front (i.e. $c/c_0 = 0{\cdot}1$) is only about 1·8 m/a after 30 years migration. Clearly, the velocity of the front will vary depending on the ratio of c/c_0 considered to be representative of the front. It would be slightly lower if defined at $c/c_0 = 0{\cdot}25$ and slightly higher if $c/c_0 = 0{\cdot}01$. However, referring to Figure 2, it can be seen that for any reasonable choice of c/c_0 the plume has moved less than 60 m in 30 years; if it was moving at the groundwater velocity it should have moved 6000 m in the same time. Thus, it is evident that contaminant is not moving at the groundwater velocity.

Effect of fracture arrangement

The theory presented in the previous section allows consideration of the effects of matrix diffusion for one, two- and three-dimensional fracture systems. Figure 3 shows the calculated contaminant plume after 30 years for three such cases. For the 1D case, contaminant is migrating along a single set of parallel fractures with a spacing ($2H_1$) of 0·05 m and fracture opening size ($2h_1$) of 20 μm giving a fracture porosity $n_f = n_b = 2h_1/2H_1 = 0{\cdot}0004$. For the 2D and 3D cases, contaminant is migrating along a vertical and horizontal set of fractures each with a spacing of

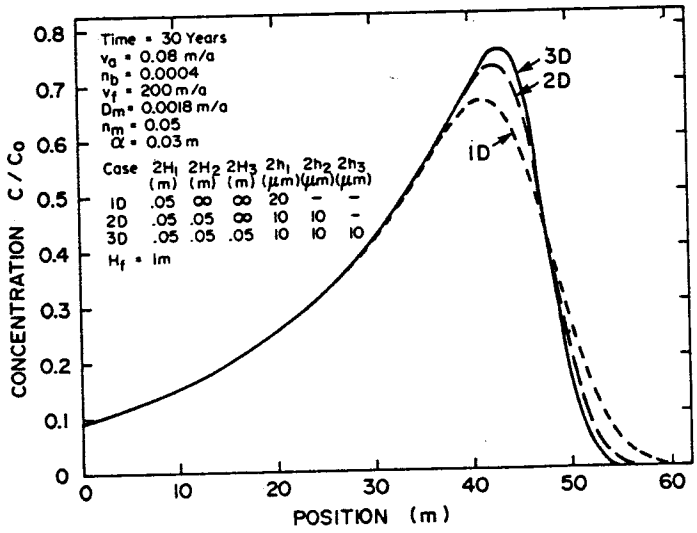

Figure 3. Effect of the nature of fracturing (1D, 2D or 3D)

0·05 m (i.e. $2H_1 = 2H_2 = 0{\cdot}05$ m) and a fracture opening size of 10 μm (i.e. $2h_1 = 2h_2 = 10$ μm) giving a fracture porosity perpendicular to the flow $n_b = (2h_1/2H_1) + (2h_2/2H_2) = 0{\cdot}0004$. The difference between the 2D and 3D analyses arises from the presence of a third fracture set orthogonal to the direction of flow in the 3D case. For 2D conditions $n_f = n_b$ since there is no third fracture set, whereas for 3D conditions $n_b = (2h_1/2H_1) + (2h_2/2H_2)$ but $n_f = (2h_1/2H_1) + (2h_2/2H_2) + (2h_3/2H_3)$.

Inspection of Figure 3 shows that the contaminant front (defined in terms of $c/c_0 = 0{\cdot}1$) moves fastest for case 1D and slowest for case 3D. This arises because in case 3D, contaminant can diffuse into the matrix of the rock from all three directions thereby allowing faster removal of contaminant from the fractures and, hence, slower migration of the plume (all other things being equal).

A consequence of the more rapid diffusion from the fractures into the rock matrix for case 3D is that equilibrium between the concentration in the rock and fracture (at a point) is reached at an earlier time than for cases 2D and 1D. Once this occurs there can be no more diffusion into the matrix at that point. Thus, at a given time, 3D diffusion into the rock matrix reduces the extent of the contaminant plume, but since the total mass of contaminant is essentially the same for cases 1D, 2D and 3D this implies that there is a greater mass of contaminant within a small volume of ground water and pore fluid, and consequently the peak concentration is higher for case 3D than for cases 2D and 1D. As can be seen from Figure 3, the peak for case 3D is approximately 76 per cent of the initial source value as compared to about 73 per cent for case 1D.

Supposing that the primary fracture set is horizontal at a spacing $2H = 0{\cdot}05$ m, the results presented in Figure 3 encompass the range of possible spacings of orthogonal vertical fractures between a close spacing of 0·05 m and no vertical fractures at all. Figure 3 demonstrates that this spacing does affect the extent of the contaminant plume and the peak impact at a given point; however the effect is not particularly large considering the wide range of vertical fracture spacings examined. This has important practical consequences in that it implies that any reasonable estimate of the secondary fracture spacings is likely to give results which are sufficiently accurate for engineering purposes and that the effect of reasonable irregularity in the secondary fracture spacing can be readily bracketed using the theory presented in the previous section.

Effect of matrix diffusion coefficient and porosity

Figures 4 and 5 show the calculated variation in concentration with position after 30 years migration for a number of combinations of matrix diffusion coefficient D_m and matrix porosity, n_m. Figure 4 gives results for a single direction of fracturing, and Figure 5 gives corresponding results for three sets of orthogonal fractures. The basic trends shown in the two sets of figures is the same. Referring to either Figure, it is seen that the velocity at which the contaminant plume moves away from the source is primarily related to the matrix porosity (for a given fracture spacing). In fact, for this case it can be seen that for both diffusion coefficients considered, reducing the matrix porosity by a factor of two, from 0·1 to 0·05, increased the velocity of the peak of the contaminant plume by a factor of two from about 0·7 *m/a* to about 1·4 *m/a*.

It is evident from Figures 4 and 5 that the peak concentration is smaller for a porosity of 0·1 than for 0·05; however these plots do not fully illustrate the effect that porosity has on attenuation. To illustrate this, Figure 6 shows the variation in concentration with time at a point 30 m from the source for the four combinations of parameters considered in Figure 4. This figure reinforces the earlier observation that a higher porosity reduces the speed of the contaminant plume and reduces the magnitude of the peak impact at a given point.

The effect of diffusion coefficient on contaminant migration is related to the time required to

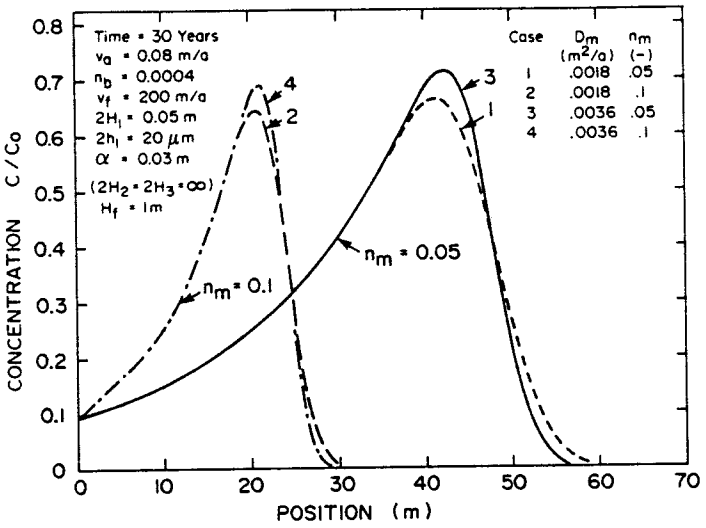

Figure 4. Effect of diffusion coefficient and matrix porosity on the contaminant plume: 1D Fracture system

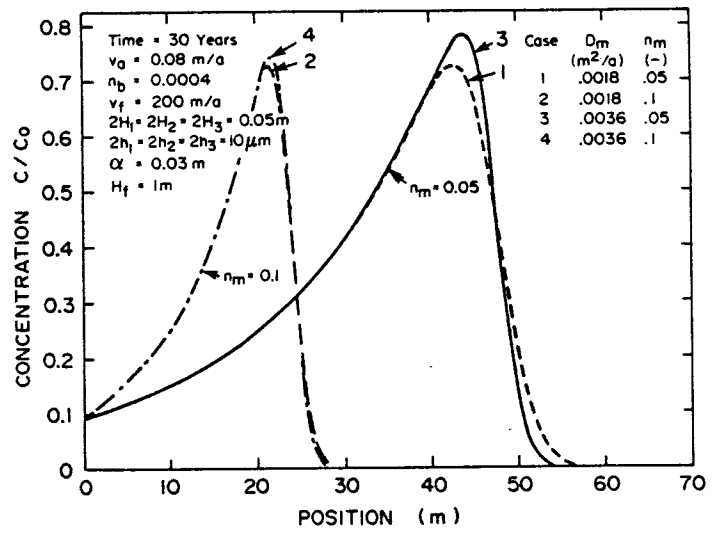

Figure 5. Effect of diffusion coefficient and matrix porosity on the contaminant plume: 3D fracture system

'saturate' the pore fluid between fractures with contaminant (i.e. in the following discussion the time to 'saturate the rock' is the time required to reach steady state for diffusion into the matix at a given point given a constant concentration in the fracture). A higher diffusion coefficient allows more rapid movement of contaminant into (and out of) the rock matrix. Thus as the contaminant moves along the fracture, the extent of the plume will be limited by diffusion into the rock matrix until the concentration in the rock between fractures reaches a value equal to the concentration in the fracture. No more contaminant can then enter the rock at this point (in fact, contaminant will

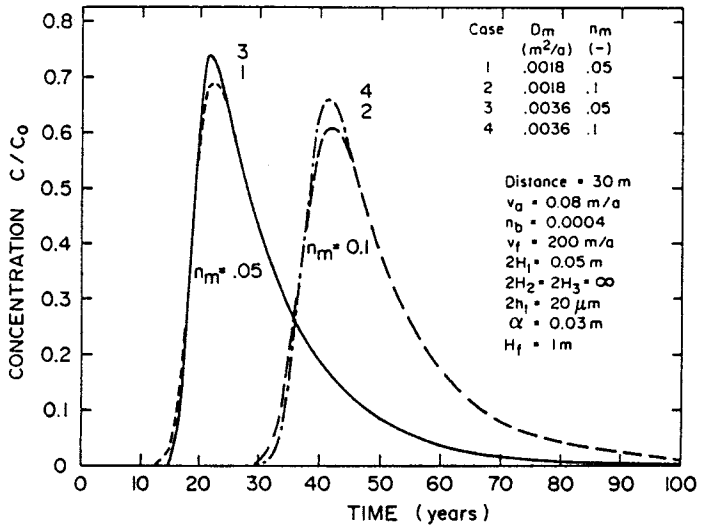

Figure 6. Effect of diffusion coefficient and matrix porosity on contaminant arrival times at a point 30 m from the source

diffuse out of the matrix once the concentration in the fracture begins to decrease). The time required to 'saturate' the matrix with contaminant at a given point is about 1 year for a single set of fractures at a spacing of 0·05 m and a diffusion coefficient of 0·0018 m^2/a and about 0·5 years for a diffusion coefficient of 0·0036 m. Since these time scales are small compared with the time being examined (i.e. 30 years), much of the rock is 'saturated' with contaminant in both cases. Under these circumstances, where saturation can occur over a significant extent of the rock in the time frame of interest, the maximum peak concentration and minimum extent of the plume will be obtained for the case where the contaminant can most quickly 'saturate' the rock between fractures. Thus, increasing the diffusion coefficient by a factor of two from 0·0018 m^2/a to 0·0036 m^2/a results in a slightly smaller plume for the higher diffusion coefficient but, since essentially the same amount of mass is involved, the peak concentration is consequently higher, as shown in Figures 4 or 5.

The effect of the time scale required to 'saturate' the rock is also evident from a comparison of Figures 4 and 5. When contaminant can diffuse into the matrix from three directions (as considered in Figure 5) as opposed to one (as considered in Figure 4), the time required to 'saturate' the rock matrix with contaminant is considerably reduced for a given diffusion coefficient (by more than a factor of two in this case). As a result, for a given combination of diffusion coefficient and matrix porosity, the extent of the contaminant plume is less for 3D diffusion (Figure 5) than for 1D diffusion (Figure 4) and the magnitude of the peak concentration is greatest for the 3D case.

Effect of fracture spacing

As illustrated in Figures 4, 5 and 6, the twofold reduction in diffusion coefficient from 0·0036 to 0·0018 m^2/a does in this case result in a modest reduction in the magnitude of the peak concentration but very little change in the velocity of the contaminant plume. However, this finding should not be extrapolated to other situations. For example, as the spacing between fractures increases, the time required to saturate the rock with contaminant also increases. When

the time required to saturate the rock becomes significant compared to the time frame of interest, then a higher diffusion coefficient may be expected to exert a different influence on the shape of the contaminant plume since, by definition, there will not have been time for contaminant to diffuse fully into the rock along most of the distance between the source and the point of interest. To illustrate this, Figure 7 shows the calculated contaminant plume for fracture spacings of 0·05 m and 0·5 m for two values of matrix diffusion coefficient (i.e. $D_m = 0{\cdot}0018\ m^2/a$ and $D_m = 0{\cdot}0036\ m^2/a$).

It is evident from Figure 7 that the spacing between the primary set of fractures is a very important parameter influencing contaminant movement. As previously noted, the times required for contaminant diffusion to 'saturate' the matrix with contaminant are about 1 year and 0·5 years for $D_m = 0{\cdot}0018$ and $0{\cdot}0036\ m^2/a$, respectively, and a spacing of $2H_1 = 0{\cdot}05$ m.

For a fracture spacing $2H_1 = 0{\cdot}5$ m, the times required to 'saturate' the matrix with contaminant at a point are of the order of 100 years and 50 years for $D_m = 0{\cdot}0018$ and $0{\cdot}0036\ m^2/a$, respectively. Thus when examining the contaminant impact at a point 30 m from the source (as shown in Figure 7) this time is significant (i.e. of the same order) as the time required for the peak contaminant impact to reach the point of interest. In this case it can be seen that the much greater time required to saturate the matrix with contaminant results in a much greater spread of contaminant along the fracture system. The time of arrival of the contaminant front, t_a (defined as the time when c/c_0 first equals 0·1) is much sooner and is far more sensitive to the magnitude of the matrix diffusion coefficient for the wider fracture spacing of 0·5 m (where $t_a = 9$ years and 16 years for $D_m = 0{\cdot}0018\ m^2/a$ and $0{\cdot}0036\ m^2/a$, respectively) than for the narrower fracture spacing of 0·05 m (where the corresponding times are $t_a = 33$ years and $t_a = 34$ years).

In this case, the larger spacing between fractures ($2H_1 = 0{\cdot}5$ m) also gives rise to a substantially smaller peak impact and earlier arrival of this impact than was calculated for the narrower fracture spacing ($2H_1 = 0{\cdot}05$ m). The primary reason for this is that on the time scale being considered, the contaminant is much more spread out along the fracture for the wider spacing and,

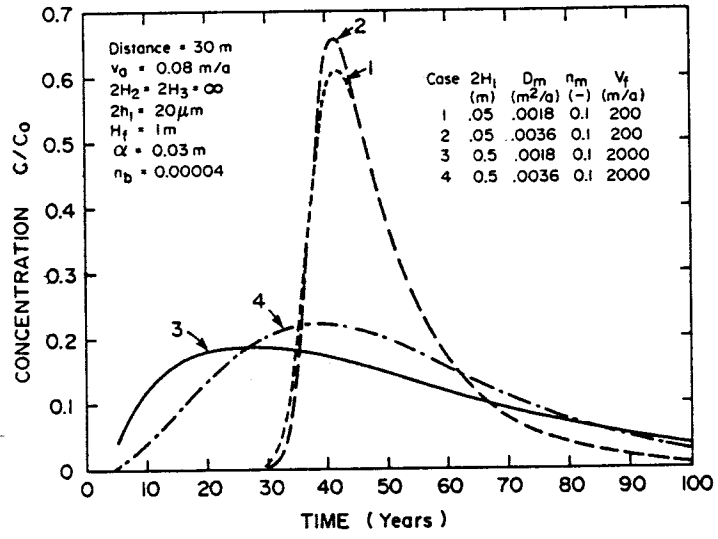

Figure 7. Effect of fracture spacing, $2H_1$, on arrival times at a point 30 m from the source

since essentially the same mass is spread over a larger volume of rock, the peak impact is correspondingly reduced.

It should be emphasized that the effect of fracture spacing on the contaminant plume is very dependent on both the mass of contaminant and the ratio time of interest to the time required to 'saturate' the matrix between fractures. Because of the complex interaction between the effect of different parameters, care should be taken not to overgeneralize from the results of any one set of analyses. Fracture spacing is clearly an important parameter and its effects, and interaction with other parameters such as distribution coefficient, will be discussed in more detail in a subsequent paper.[15]

Effect of dispersivity

Figures 8 and 9 show the calculated variations in concentration with time at a point 30 m from the contaminant source for 1D and 3D fracture sets, respectively. In both cases, results are shown for three different values of dispersivity α (i.e. 0·03, 0·3 and 3 m) which correspond to 0·1, 1 and 10 per cent of the travel distance. A small dispersivity (implying very little mechanical dispersion due to irregularities in the fracture system) gives the greatest impact (all other things being equal). Higher dispersivities give rise to a more extensive contaminant plume and, since the mass of contaminant is spread over a greater volume of rock, a smaller peak impact at a given point.

Comparing the results given for the 1D and 3D fracture networks (Figures 8 and 9), it can be seen that the nature of the fracture network does not significantly influence the general effect of increasing dispersivity; however it should be noted that this observation assumes that one would have the same dispersivities for both systems. In reality, if one were to compare contaminant parameters for two fractured rock systems having the same bulk hydraulic conductivity, one would expect that if the fracture system was essentially one dimensional, the dispersivity would be quite different than if the fracture system was largely three dimensional and so, in practice, the analysis of a 3D system would invariably involve the use of a different dispersivity than the analysis of a 1D system.

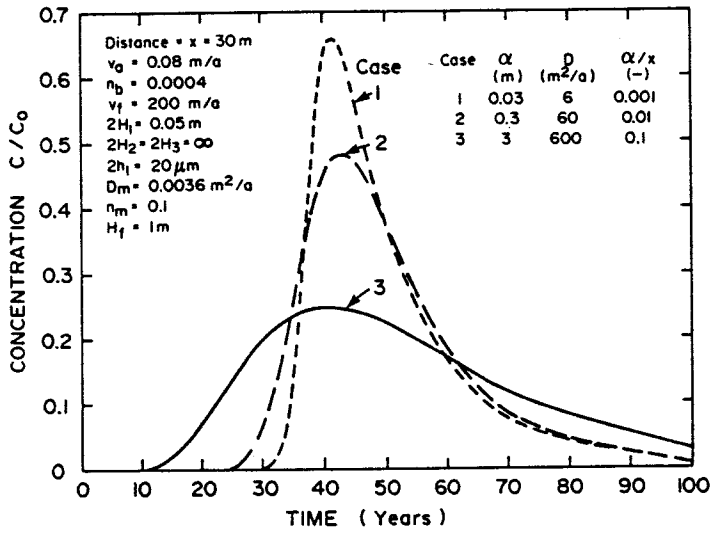

Figure 8. Effect of dispersivity, α, on arrival times at a point 30 m from the source: 1D fracture system

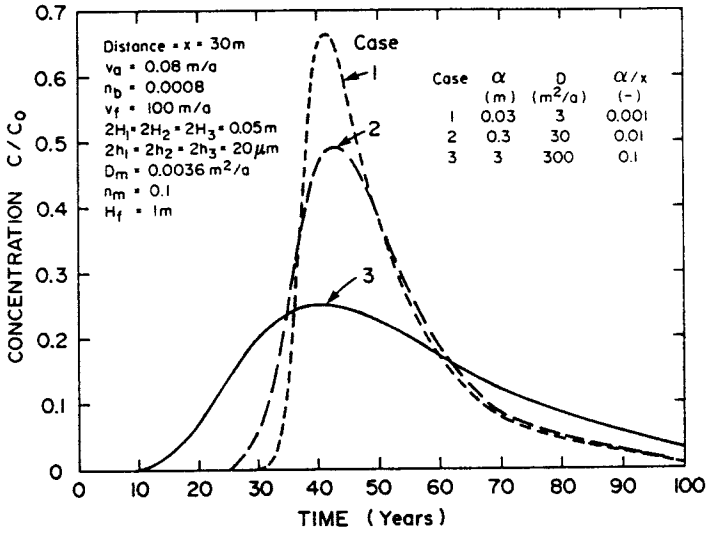

Figure 9. Effect of dispersivity, α, on arrival times at a point 30 m from the source: 3D fracture system

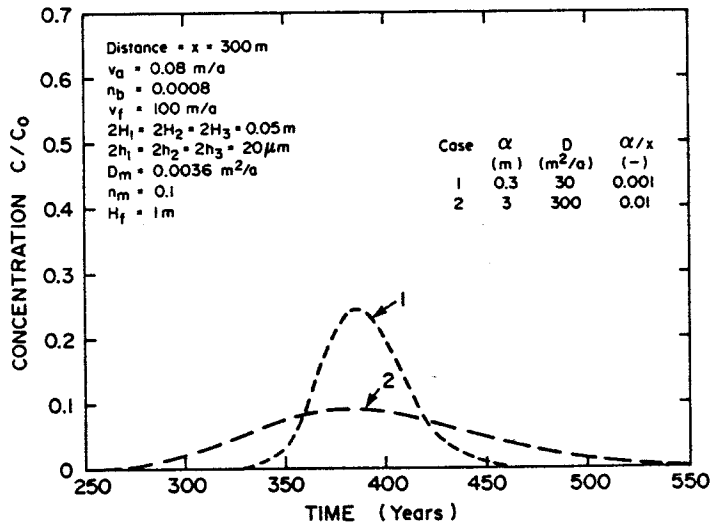

Figure 10. Effect of dispersivity, α, on arrival times at a point 300 m from the cource: 3D fracture system

Dispersivity is generally considered to increase with distance from the source, at least until the distance involved is large compared to the scale of the non-homogeneities of the flow system which give rise to the dispersion process.[13] Figure 10 shows the variation in concentration with time at a point 300 m from the source for a 3D fracture system. These results may be compared with the corresponding results for a point at 30 m given in Figure 9. As contaminant moves from the 30 m monitoring point to the 300 m point, it spreads out over a much larger volume of rock, and consequently if one compares the peak impact calculated for a given dispersivity (e.g. 3 m) at the two locations it is seen that there is substantial attenuation as contaminant moves away from the

source. If one were to argue that the dispersivity should be a function of distance, then the attenuation would become even more significant. For example, if one considered the dispersivity to be a linear function of distance (say one per cent of the travel distance: $\alpha/x = 0{\cdot}01$) then one could compare the results given for curve 2 in Figures 9 and 10 (i.e. for $\alpha/x = 0{\cdot}01$ and hence $\alpha = 0{\cdot}3$ m in Figure 9 and $\alpha = 3$ m in Figure 10) and would see that the peak impact at the monitoring point is reduced by more than a factor of five between the 'monitoring' points at 30 m and 300 m.

Effect of fracture opening size and dispersivity

Figures 8 and 9 present results for the same Darcy flow through a 1D and 3D fracture system. If the fracture opening size is the same both vertically and horizontally, then this implies that the fracture porosity for the 3D fracture system is twice that for the 1D system ($n_b = 0{\cdot}0008$ in Figure 9 versus 0·0004 in Figure 8). For the same Darcy flow, this implies that there is a factor of two difference in groundwater velocity v_f (i.e. 100 m/a in Figure 9 and 200 m/a in Figure 8). However, despite this significant difference in groundwater velocity, comparison of the curves in Figures 8 and 9 for corresponding dispersivities α indicates very similar results, and indeed the time of arrival and magnitude of the contaminant peak is almost identical for the two cases. This has important practical implications since it implies that uncertainty as to the fracture porosity and groundwater velocity has very little effect on prediction of contaminant transport.

In fact, the fracture opening size is one of the most difficult parameters to determine and it is of interest to explore the implication of uncertainty regarding this parameter since the fracture porosity and, hence, groundwater velocity both depend on this parameter.

Figure 11 shows the calculated contaminant plume after 30 years migration for five cases involving a 3D fracture system. All cases assume the same Darcy velocity. In cases 1, 2 and 3 the fracture opening size is varied between 10 μm and 40 μm giving a consequent fourfold variation in groundwater velocity from 200 m/a to 50 m/a. For a given dispersivity of 0·03 m it can be seen that this fourfold variation in opening size and ground-water velocity does slightly change the contaminanat plume; however this change is of no practical significance. In each case, the peak of

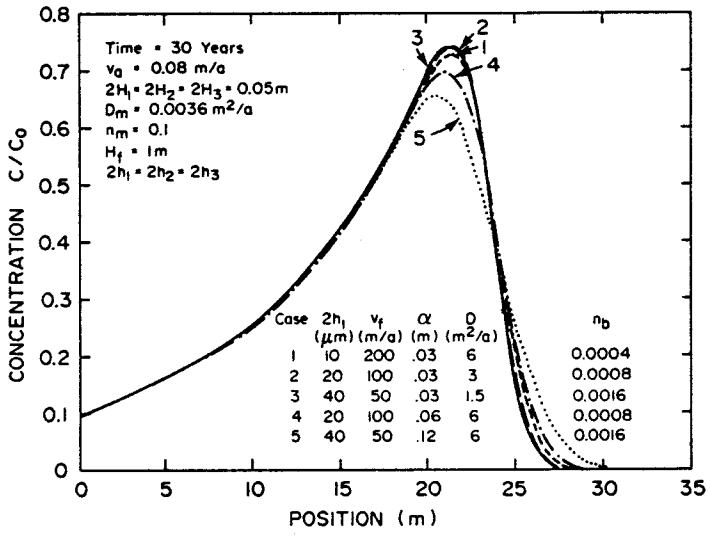

Figure 11. Effect of fracture opening size, $2h_1$, and dispersivity, α, on the contaminant plume

the contaminant plume is moving at a velocity of 0·7 m/a irrespective of whether the groundwater velocity is 50 or 200 m/a.

The coefficient of hydrodynamic dispersion, D, is often assumed to be linearly proportional to the ground-water velocity v_f (i.e. $D = \alpha v_f$, where α is the dispersivity). In the comparison of cases 1, 2 and 3 above, it has been assumed that the dispersivity remained constant ($\alpha = 0{\cdot}03$ m) and hence the coefficient of hydrodynamic dispersion did vary by a factor of four due to the variation in groundwater velocity. It would be reasonable to argue that the dispersivity was a function of the travel distance as assumed above. However, it may also be reasonable to argue that really it is the coefficient of hydrodynamic dispersion that is a function of distance only. To examine the implications of this assumption, cases 1, 4 and 5 (Figure 11) represent results for fracture opening sizes of 10, 20 and 40 μm and a single coefficient of hydrodynamic dispersion of 6 m^2/a. In this case, it can be seen that increasing the assumed fracture opening size from 10 to 40 μm does result in a change in the contaminant plume primarily due to the fact that for the high opening size there is (relatively speaking) a fourfold increase in the ratio of the coefficient of hydrodynamic dispersion to groundwater velocity (i.e. even though the coefficient of hydrodynamic dispersion remains constant there is more potential for spreading of contaminant at lower groundwater velocities). Nevertheless, from a practical standpoint, it can be seen that a fourfold variation in average fracture opening size (and hence groundwater velocity) does not significantly influence the speed of contaminant transport or the peak impact (which varies by less than 10 per cent for a fourfold variation in opening size) even under the most unfavourable assumptions. This clearly implies that uncertainty as to the precise details concerning fracture opening size is not going to have a significant effect on prediction of contaminant transport.

Effect of Darcy velocity

It is evident from the preceding discussion that the ground-water velocity is of secondary significance when predicting the rate of contaminant migration through fractured porous media. This is fortunate since the groundwater velocity is very sensitive to changes in opening size and hence is difficult to estimate and may vary substantially within a given mass of rock. A more readily determined parameter is the Darcy velocity (Darcy flux) which represents the volume of water moving through the fractured rock mass per unit area per unit time. This quantity can be deduced from the measured bulk hydraulic conductivity and gradient within the fractured rock mass.

Figure 12 shows the effect of varying the Darcy velocity on the contaminant plume after 30 years migration. Results are given for Darcy velocities of 0·04 and 0·08 m/a and it can be seen that doubling the Darcy velocity results in an approximate doubling of the velocity of the peak of the plume. Curves 1 and 2 show the effect of increasing the Darcy velocity while maintaining a constant dispersivity, α. Curves 3 and 4 show the effect of increasing the Darcy velocity while maintaining a constant coefficient of hydrodynamic dispersion. Clearly, the assumption regarding what happens to dispersion when the Darcy velocity changes does have some impact on the contaminant plume; however the primary effect is clearly due to a change in Darcy velocity and dispersion is a secondary consideration.

The results presented in Figure 12 were obtained by varying the Darcy velocity for a given fracture distribution and fracture porosity. Thus the groundwater velocity varies in proportion to the Darcy velocity. To emphasize the point that it is the Darcy velocity (flux) and not the ground-water velocity which is the primary control on contaminant transport, the results in Figure 13 were obtained by varying the Darcy velocity and fracture porosity such that the groundwater velocity remained constant at 100 m/a. Comparing Figures 12 and 13 (especially comparing

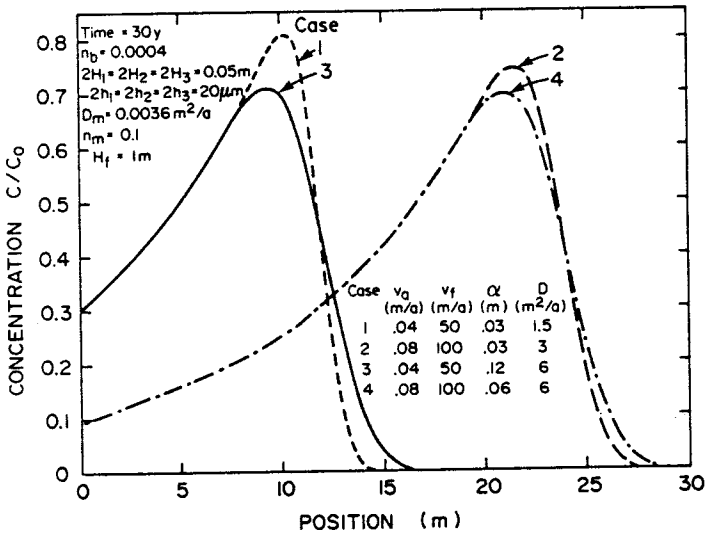

Figure 12. Effect of Darcy velocity on contaminant plume (constant fracture porosity)

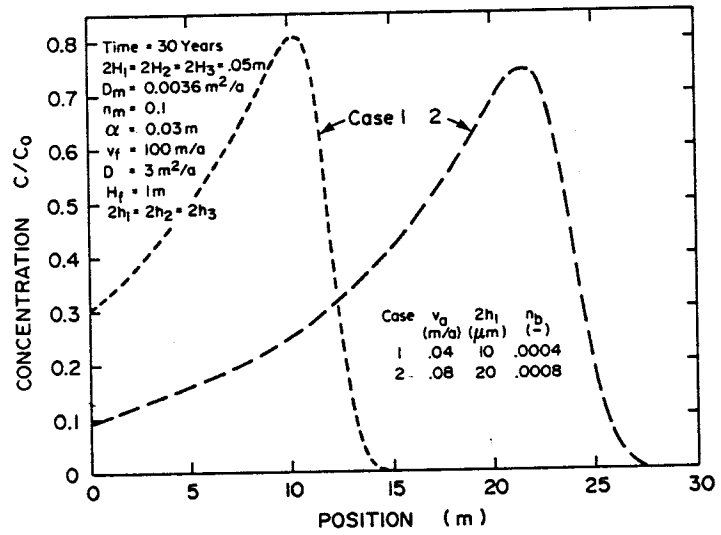

Figure 13. Effect of Darcy velocity on the calculated contaminant plume (constant ground-water velocity v_f)

curve 1 on both Figures) it is seen that for a given dispersivity and Darcy velocity the difference in ground-water velocity between 50 m/a and 100 m/a has no significant effect on the contaminant plume, whereas it is seen from Figure 13 that for a given dispersivity and groundwater velocity, the difference in Darcy velocity between 0·04 and 0·08 m/a approximately doubles the movement of the peak of the contaminant plume. Thus, it is the Darcy velocity and not the groundwater velocity which controls the movement of the contaminant plume and the impact on groundwater quality.

CONCLUSIONS

A new semi-analytical solution for contaminant transport of conservative contaminant species in fractured media having a regular two- or three-dimensional fracture network has been presented. The application of the technique and some of the practical implications arising from an examination of contaminant migration in fractured systems are then discussed. For a conservative contaminant and the range of parameters considered in this study, it is concluded that

1. The rate of contaminant transport does not significantly depend on the groundwater velocity. The rate of movement and the degree of attenuation do, however, greatly depend on the fracture spacing, matrix porosity, dispersivity, Darcy velocity (i.e. Darcy flux) and the mass of contaminant available for transport.
2. For a given spacing between the primary fractures, consideration of the spacing between the secondary fractures reduces the calculated velocity of the leading edge of the contaminant plume but increases the calculated maximum impact of the plume.
3. Any reasonable estimate of secondary fracture spacing is likely to give results which are sufficiently accurate for engineering purposes.
4. The larger the matrix porosity, the slower will be the contaminant transport velocity and the greater the attenuation.
5. The magnitude of the matrix diffusion coefficient needs to be known reasonably well when the time scale of interest is similar to or greater than the time required to reach a steady state due to diffusion into the rock matrix at a point.
6. Fracture opening size is only important in so far as it influences the hydraulic conductivity of the rock mass and, accordingly, the Darcy velocity. Any combination of fracture opening sizes which gives rise to a given hydraulic conductivity will give rise to a contaminant impact which, for all practical purposes, is the same. The effect of uncertainty regarding the magnitude of opening size upon the ground-water velocity does not have any significant effect on the prediction of contaminant migration.

APPENDIX

The mass of leachate which has entered the matrix can be calculated from the concentration with each block, and thus if V_m denotes the region occupied by the blocks, then recalling that the width of the fissures is very small relative to the minimum dimension of the block it follows that

$$q = \frac{\int n_m c_m \, dV_m}{\int 1 \, dV_m} \tag{14}$$

where n_m denotes the porosity of the matrix and c_m the concentration in the matrix.

It will be assumed that there is no advective transport within the matrix and thus that

$$D_m \nabla^2 c_m = \frac{\partial c_m}{\partial t} \tag{15}$$

where D_m is the coefficient of molecular diffusion within the matrix.

It follows upon application of a Laplace transform that

$$D_m \nabla^2 \bar{c}_m = s\bar{c}_m \tag{16}$$

There are now three cases to consider.

Case 1

First, suppose there is only a single set of fissures (set 1), then because of the assumed conditions in the landfill there is no variation of concentration with respect to y. Also, the variation of concentration is likely to be relatively slow along the fissures (x direction) when compared with the variation between adjacent fissures (z direction), and thus to sufficient accuracy the concentration within the fissures satisfies the equation

$$D_m \frac{\partial^2 \bar{c}_m}{\partial z^2} = s\bar{c}_m \tag{17}$$

and the boundary conditions

$$\bar{c}_m = \bar{c}_f \quad z = \pm H_1$$

where it has been convenient to introduce a local set of axes at the centre of the block.

It thus follows, employing a finite Fourier cosine transformation, that

$$\bar{c}_m = \bar{c}_f\left(1 - 2\sum_{j=1}^{\infty} \frac{s\cos(\alpha_j z)}{(s+\alpha_j^2 D_m)} \frac{\sin\alpha_j H_1}{\alpha_j H_1}\right) \tag{18}$$

where

$$\alpha_j = \left(j - \frac{1}{2}\right)\frac{\pi}{H_1}$$

It now follows from the Laplace transform of equation (14) that

$$\bar{q} = \bar{c}_f \bar{\eta} s \tag{19}$$

where

$$\bar{\eta} = n_m\left[1 - 2\sum_{j=1}^{\infty} \frac{1}{(\alpha_j H_1)^2} \frac{s}{(s+\alpha_j^2 D_m)}\right]$$

Case 2

Let us now assume that there are two sets of fissures (sets 1 and 2); then again observing that variation in the x direction is likely to be far slower than with the matrix we see that

$$D_m\left(\frac{\partial^2 \bar{c}_m}{\partial y^2} + \frac{\partial^2 \bar{c}_m}{\partial z^2}\right) = s\bar{c}_m \tag{20}$$

with

$$\bar{c}_m = \bar{c}_f,\ z = \pm H_1 \qquad \bar{c}_m = \bar{c}_f,\ y = \pm H_2 \tag{21}$$

where again it has been convenient to introduce a local set of axes at the centroid of the block.

Again, a straightforward application of finite Fourier transforms yields

$$c_m = c_f\left\{1 - 4\sum_{j=1}^{\infty}\sum_{k=1}^{\infty} \frac{s\cos(\alpha_j z)\cos(\beta_k y)\sin(\alpha_j H_1)\sin(\beta_k H_2)}{(\alpha_j H_1)(\beta_k H_2)[s+(\alpha_j^2+\beta_k^2)D_m]}\right\} \tag{22}$$

with

$$\beta_k = \left(k - \frac{1}{2}\right)\frac{\pi}{H_2}$$

whereupon

$$\bar{q} = \bar{c}_f \bar{\eta} s \tag{23}$$

where

$$\bar{\eta} = n_m \left\{ 1 - 4 \sum_{j=1}^{\infty} \sum_{k=1}^{\infty} \frac{1}{(\alpha_j H_1)^2 (\beta_k H_2)^2} \frac{s}{[s + (\alpha_j^2 + \beta_k^2) D_m]} \right\}$$

Case 3

Finally, if there are three sets of fissures and it is observed that variation in the direction of transport is relatively slow compared to the dimensions of the block then, adopting local axes at the centroid of the block, it is found that

$$\bar{c}_m = \bar{c}_f \left\{ 1 - 8 \sum_{j=1}^{\infty} \sum_{k=1}^{\infty} \sum_{l=1}^{\infty} \frac{s \cos(\alpha_j z) \cos(\beta_k y) \cos(\gamma_l x) \sin(\alpha_j H_1) \sin(\beta_k H_2) \sin(\gamma_l H_3)}{(\alpha_j H_1)(\beta_k H_2)(\gamma_l H_3)[s + D_m(\alpha_j^2 + \beta_k^2 + \gamma_l^2]} \right\} \tag{24}$$

with $\gamma_l = (l - \frac{1}{2}) \dfrac{\pi}{H_3}$

and that

$$\bar{q} = \bar{c}_f \bar{\eta} s$$

with

$$\bar{\eta} = n_m \left\{ 1 - 8 \sum_{j=1}^{\infty} \sum_{k=1}^{\infty} \sum_{l=1}^{\infty} \frac{1}{(\alpha_j H_1)^2 (\beta_k H_2)^2 (\gamma_l H_3)^2} \frac{s}{[s + D_m(\alpha_j^2 + \beta_k^2 + \gamma_l^2)]} \right\} \tag{25}$$

ACKNOWLEDGEMENTS

Funding of the general programme of research into contaminant migration of which this paper forms a part has been provided by the Natural Sciences and Engineering Research Council of Canada under grant No. A1007. The computations reported in this paper were performed on a microcomputer which was purchased with a grant from the University of Western Ontario Foundation Inc.

REFERENCES

1. R. A. Freeze and J. A. Cherry, *Groundwater*, Prentice-Hall Inc. Englewood Cliffs, New Jersey, 1979.
2. G. E. Grisak and J. F. Pickens, 'Solute transport through fractured media, 1. The effect of matrix diffusion', *Water Resources Research*, **16**, (4), 719–730 (1980).
3. G. E. Grisak, J. F. Pickens and J. A. Cherry, 'Solute transport through fractured media, 2. Column study of fractured till', *Water Resources Research, Vol.* **16**, 731–739 (1980).
4. R. W. Gillham and J. A. Cherry, 'Contaminant migration in saturated unconsolidated geologic deposits', Geophysical Society of America, *Special Paper* 189, 1982, pp. 31–62.
5. R. K. Rowe, 'Contaminant migration through groundwater: the role of modelling in the design of barriers', *Canadian Geotechnical Journal*, **25**, (4), 778–798 (1988).
6. P. S. Huyakorn, B. H. Lester and J. W. Mercer, 'An efficient finite element technique for modelling transport in fractured porous media, 1. Single species transport', *Water Resources Research*, **19**, (3), 841–854 (1983).
7. I. Neretnieks, 'Diffusion in the rock matrix: an important factor in radio nuclide retardation', *J. Geophys. Res.* **85**, (B8), 4379–4397 (1980).
8. D. H. Tang, E. O. Frind, and E. A. Sudicky, 'Contaminant transported in fractured porous media: analytical solution for a single fracture', *Water Resources Research*, **17**, 555–564 (1981).
9. E. A. Sudicky and E. O. Frind, 'Contaminant transport in fractured porous media: analytical solution for a system of parallel fractures', *Water Resources Research*, **18**, 1634–1642 (1982).
10. J. A. Barker, 'Laplace transform solutions for solute transport in fissured aquifers', *Advanced Water Research*, **5** (2), 98–104 (1982).

11. L. Moreno and A. Rasmuson, 'Contaminant transport through a fractured porous rock: impact of the inlet boundary condition on the concentration profile in the rock matrix', *Water Resources Research*, **22**, (12), 1728–1730 (1986).
12. R. K. Rowe, and J. R. Booker, 'Modelling of contaminant movement through fractured or jointed media with parallel fractures', *Proceedings of 6th International Conference on Numerical Methods in Geomechanics*, Innsbruck, April 1988, pp. 855–862.
13. E. O. Frind, E. A. Sudicky and S. L. Schellenberg, 'Micro-scale modelling in the study of plume evolution in heterogeneous media', *Stochastic Hydrol. Hydraul.*, **1**, 263–279 (1987).
14. A. Talbot, 'The accurate numerical integration of Laplace transforms', *J. Inst. Maths. Applics.*, **23**, 97–120 (1979).
15. R. K. Rowe and J. R. Booker, 'A semi-analytic model for contaminant migration in a regular two- or three-dimensional fractured network: reactive contaminants', *Int. j. numer. anal. methods Geomech.*, to appear.